Single Pulse Laser-Induced Phase Transitions of PLD-Deposited $Ge_2Sb_2Te_5$ Films

*Hongbing Lu, Erik Thelander, Jürgen W. Gerlach, Ulrich Decker, Benpeng Zhu, and Bernd Rauschenbach**

Phase transformations between amorphous and crystallized states are induced by irradiation with a single nanosecond laser pulse in $Ge_2Sb_2Te_5$ films grown by pulsed laser deposition. By adjusting the laser fluence, the two different phases are obtained and can be distinguished by their different optical reflectivity. The effect of laser fluence on the crystalline nature of the films is studied in detail. Large structural differences between the laser-irradiated and thermally annealed films are revealed, due to the high heating rate and short duration of the laser pulse. X-ray reflectivity measurements show a density increase of 3.58% upon laser-induced crystallization.

1. Introduction

Chalcogenide-based alloys have found a wide use in optical data storage[1] and are of increasing interest for applications in non-volatile memories. The basic principle of the optical memory storage is based on the reversible transformations between the disordered amorphous and ordered crystalline phases.[2] Writing of bits corresponds to the formation of small amorphous marks in a crystalline matrix whereas the recrystallization of the amorphous spots leads to the erasure of information. In the writing process, a high-intensity laser pulse is used to heat the phase-change layer locally above its melting temperature. After the laser pulse, the molten area cools rapidly with a rate higher than 10^9 K/s and is quenched into the amorphous state.[1,3] In the erasing process, a laser pulse with intermediate power is used to heat the amorphous layer above the crystallization temperature but below the melting temperature, which brings the material back to the crystalline phase. Utilizing a significantly different optical reflectivity between the amorphous and crystalline states, data bits can be read by monitoring the local changes in the reflectivity of the media with a low power laser beam.

Among various phase-change materials, the Ge–Sb–Te family, and particularly $Ge_2Sb_2Te_5$ (GST), is the most distinguished one because of its short crystallization times (tens of nanoseconds), prominent reflectivity contrast, excellent reversibility, large cycle number of reversible transitions, and high archival lifetime of more than ten years.[1,4,5] In the past years, extensive experimental studies on phase transformation from the amorphous to crystalline states induced by thermal annealing have been reported,[5–9] where annealing times between 5 minutes and 2 hours were typically applied to crystallize the GST films. Additionally, laser-induced crystallization of GST films has also been demonstrated.[10–14] Amorphization of GST films (46 nm in thickness) induced by nanosecond laser pulses with a laser spot size of 100×59 μm^2 has been reported by Siegel et al.,[10] who studied the optical reflectivity of the films. Using picosecond laser pulses with a laser spot diameter of 240 μm, Siegel et al.[13] also reported the reversible phase transformation of GST films (50 nm in thickness), and investigated the optical reflectivity of films during crystallization and amorphization. Femtosecond laser pulses with a laser spot diameter of 200 μm was also used to crystallize GST films by Kong et al.,[14] who focused on the Raman properties of films with increasing laser fluence (for definition of fluence, see Experimental Section). These previous reports on laser-induced crystallization, however, were mainly focused on the optical properties of the films with thin thicknesses (10–50 nm) and small laser spot sizes.[10,11,13,14] The detailed structural information is thus lacking since it is very hard to detect X-ray diffraction (XRD) peaks for such thin films with small laser-crystallized area. Compared to the annealing-induced crystallization, laser-induced crystallization has much higher heating/cooling rates (larger than 10^9 K/s)[15] due to the short pulse duration. It is therefore of great value to get detailed structural information from laser-crystallized GST films, since it resembles practical application more, compared to that for the thermally annealed films with long annealing times.

Dr. H. B. Lu, E. Thelander, Dr. J. W. Gerlach, Dr. U. Decker, Prof. B. Rauschenbach
Leibniz Institute of Surface Modification (IOM)
Permoserstr. 15, D-04318 Leipzig, Germany
E-mail: bernd.rauschenbach@iomleipzig.de
Dr. H. B. Lu, Dr. B. P. Zhu
Ministry-of-Education Key Laboratory for the Green Preparation and Application of Functional Materials
Faculty of Materials Science and Engineering
Hubei University
Wuhan 430062, China
Dr. B. P. Zhu
School of Optical and Electronic Information
Huazhong University of Science and Technology
Wuhan 430074, China
Prof. B. Rauschenbach
University Leipzig
Institute for Experimental Physics I
Linnéstr. 5, D-04308 Leipzig, Germany

DOI: 10.1002/adfm.201202665

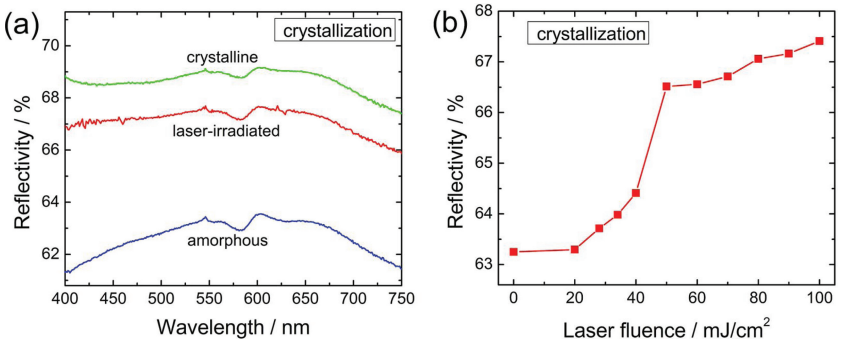

Figure 1. a) Optical reflectivity of an as-deposited film, a crystalline film induced by thermal annealing at 240 °C for 20 min, and a crystalline film induced by laser irradiation of the as-deposited film with a single nanosecond laser pulse at 100 mJ/cm^2. b) Optical reflectivity at 650 nm obtained after irradiation of amorphous films as a function of laser fluence.

For the fabrication of GST thin films, magnetron sputtering is typically employed.[3,8,16] Other methods, such as metal organic chemical vapor deposition,[17] thermal evaporation,[18] and solution-phase deposition,[19] are also used. Pulsed laser deposition (PLD), as a common deposition method, can be used to achieve the desired film properties by easily adjusting some parameters, such as growth temperature, pressure, laser fluence, laser spot area, and target-substrate distance. In particular, PLD is capable of deposition of films with unusual composition, and stoichiometric transfer of a target material to the films. In this paper, nanosecond-PLD is used as a deposition technique to fabricate GST films on Si substrates. A reversible phase transformation of GST films upon pulsed laser irradiation is demonstrated. Both optical and structural properties of the films are investigated by combination of optical reflectivity and XRD measurements. The effect of laser fluence on optical and structural properties as well as density change of these GST films is presented, which are of crucial importance for the performance of a phase-change material. In addition, a comparison of XRD results between the annealing-induced and laser-induced crystalline films is carried out, showing large differences in structural information.

2. Results and Discussion

Optical reflectivity measurements can provide an indirect observation of the structural evolution process for phase-change materials. **Figure 1**a shows the optical reflectivity of three GST films: a film deposited at room temperature, a crystalline film induced by thermal annealing at 240 °C for 20 min, and a film obtained by a single nanosecond laser pulse irradiation on the as-deposited film with a fluence of 100 mJ/cm^2. According to XRD results, the as-deposited and annealed films are in amorphous and crystalline face-centred-cubic (fcc) states, respectively. The optical reflectivity of the amorphous film is in the range from 61.3 to 63.5%, when the wavelength increases from 400 to 750 nm. In contrast, the reflectivity of the fcc film is in the range from 67.3 to 69.2%, much higher than that of the amorphous film. For the laser-irradiated film, the optical reflectivity is in the range from 65.9 to 67.7%, which is close to that of the fcc film annealed at 240 °C. This suggests that a crystalline state has formed in amorphous GST films after nanosecond laser irradiation, which will be further confirmed by XRD. It is also noted that there are features in the irradiated spectrum which are absent in the thermally annealed one. Apart from the phase changes which is a key factor determining the reflectivity of GST films, some other factors, such as surface roughness, may also affect the reflectivity of GST films with otherwise same structure.[20] Therefore, the slight difference between the thermally annealed and laser-irradiated films could be due to the increased surface roughness of the laser-irradiated film (RMS 0.219 nm for thermally annealed film compared to RMS 0.896 nm for laser irradiated film, see Supporting Information, Figure S1b,c).

Siegel et al.[10] claimed that crystallization of an as-deposited amorphous film can not be achieved with a single nanosecond laser pulse, while our result demonstrates that it is possible to crystallize PLD-deposited amorphous GST films by a single nanosecond laser pulse with short pulse duration of 20 ns. The crystallization of GST films is known to be a nucleation-dominant process.[21,22] Previous report has shown that a minimum time of 100 ns ± 10 ns was needed for stable crystalline nuclei to form and grow in an as-deposited amorphous GST film, while the complete crystallization of melt-quenched amorphous bits was possible in 10 ns due to the presence of quenched-in nuclei inside the amorphous bits.[23] It should be emphasized that our result is not in conflict with the reported minimum crystallization time for an as-deposited amorphous film, although a much shorter pulse duration of 20 ns is used in our case. This is due to the fact that the induced phase transformations may last longer than the pulse duration. Surprisingly, this fact is neglected in most of the reports. A direct comparison with shorter pulse durations, i.e., picosecond and femtosecond pulses is not completely valid, due to the absence of melting and recalescence phenomena when using picosecond or femtosecond laser pulses,[24] but recent literature reports a crystallization time of 10 ns for a picosecond laser pulse-induced crystallization of as-deposited GST films with a laser duration of 30 ps.[24]

In order to clarify the detailed effect of laser fluence on phase transition, a series of fluence-dependent reflectivity measurements on GST films was performed. The optical reflectivity is recorded at the practically often used wavelength of 650 nm, as presented in Figure 1b. At fluences ≤20 mJ/cm^2, no obvious reflectivity change can be observed. As laser fluence increases, a continuous and prominent increase in reflectivity can be seen up to ca. 50 mJ/cm^2. With further increase of the fluence from 50 to 100 mJ/cm^2, only a slight further increase in reflectivity is registered. The highest reflectivity is thus found to be 67.4% at a fluence of 100 mJ/cm^2. From these results, the threshold for a measurable reflectivity increase upon irradiation with a single nanosecond pulse is ≈20 mJ/cm^2. Above this fluence threshold, one single laser pulse heats the film above its crystallization temperature. The atoms thus become increasingly mobile and reach the energetically favorable crystalline state, leading to a

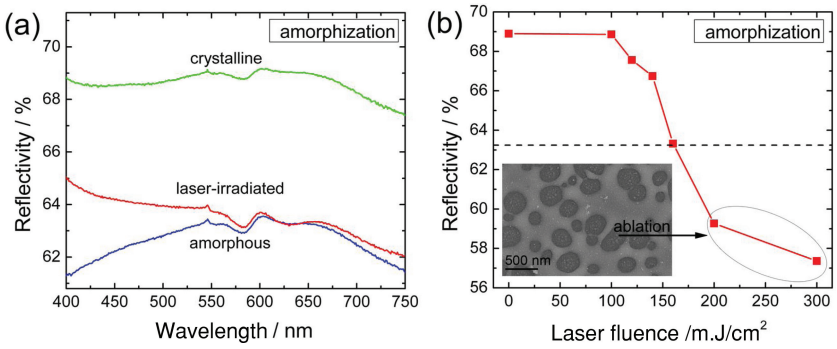

Figure 2. a) Optical reflectivity of an as-deposited film, an annealing-induced crystalline film, and an amorphous film induced by laser irradiation of the crystalline film with a single nanosecond laser pulse at 160 mJ/cm^2. b) Optical reflectivity at 650 nm obtained after irradiation of crystalline films as a function of laser fluence. The dashed line and inset picture in (b) show the reflectivity of amorphous films and SEM image of laser ablated area at high fluences, respectively.

partial crystallization of the film. With the increase of laser fluence, the extent of crystallization increases, corresponding to the increase of film reflectivity.

To correlate the thermally annealed films and the laser-irradiated films, one can estimate the temperature in the film induced by laser irradiation using the differential equation for heat conduction. If the laser radiation is spatially uniform, the equation can be written in terms of the temperature distribution $T(x,t)$ at the depth x and radiation time t.[25,26] An analytical solution of the equation is possible under the assumptions that 1) the thermal and optical parameters are independent on temperature, 2) the laser power is constant, and 3) the sample thickness is infinite (details see ref. [25,26]). For example, the temperature at the surface after a 20 ns laser pulse and an energy density of 20 mJ/cm^2 is $T(x = 0, 20\ \text{ns}) = 807$ K (534 °C), where the parameters of the GST material are assumed to be constant values (thermal conductivity is 0.582 W/mK, reflectivity is 0.65, heat capacity is 1.29 J/cm^{3}K and the density is 5.5 g/cm^3). Although this phase-change temperature is obviously much higher than the value (140 °C) of the film induced by thermal annealing,[5] it is consistent with the recent report that the crystallization temperature from the amorphous to fcc phase increases with the increase of heating rate, where a crystallization temperature of 356.5 °C was declared at a heating rate of 4×10^4 K/s.[27]

Moreover, amorphization of a crystalline film can also be achieved with a single nanosecond laser pulse irradiation. As displayed in **Figure 2**a, the annealing-induced crystalline film possesses a high optical reflectivity within the measured area. After irradiation by a single laser pulse at 160 mJ/cm^2, the reflectivity decreases significantly, corresponding well to a reflectivity level with that of the amorphous phase. Upon irradiation with a single pulse with 100 mJ/cm^2 the reflectivity is increased to the original level, hence we can rule out that the drop in reflectivity is due to other effects than phase transformation, i.e., ablation. This also show that by using a single laser pulse fluence of 160 mJ/cm^2, and 100 mJ/cm^2 the GST film can be repeatedly transformed between a crystalline and an amorphous state. The reflectivity at 650 nm obtained after irradiation of crystalline films as a function of laser fluence is further shown in Figure 2b. It can be clearly discerned that at fluences >100 mJ/cm^2, amorphization of the crystalline film occurs. The amorphization extent increases with the increase of laser fluence, and the highest extent, i.e., complete amorphization of the films is observed at a fluence of 160 mJ/cm^2. When the fluence increases to much higher values (≥200 mJ/cm^2), the reflectivity of the laser-irradiated films, on the contrary, drops much below the value of amorphous films. This can be attributed to ablation of the film surface, as verified by the scanning electron microscopy (SEM) image in the inset of Figure 2b. Holes with sizes in the range from 100 to 500 nm are clearly visible.

XRD measurements were performed to verify the observations described above and to obtain detailed structural information about the films. **Figure 3**a presents the evolution of XRD patterns of films with an increase of the laser fluence. To obtain more diffracted intensity for structural analysis, thicker films (600 nm) were used for the XRD measurements. In each case, the films were irradiated by a single nanosecond laser pulse. The corresponding laser fluences are denoted in Figure 3a. The diffraction pattern of the as-deposited film shows no obvious peaks, except for the Si(200) reflection from the substrate, confirming an amorphous state of GST films after deposition. Crystalline diffraction peaks, which are related to the (200) and (220) lattice planes of the metastable fcc phase, emerge for the film irradiated with a laser fluence of 40 mJ/cm^2. Another peak, the fcc (111) reflection appears at higher fluences (e.g., 100 mJ/cm^2). It should be pointed out that although partial crystallization of films is confirmed for fluences between 20 and 40 mJ/cm^2 from optical reflectivity measurements, XRD peaks of the crystalline phase can not be detected due to the low fraction of the crystalline phase below the fluence of 40 mJ/cm^2. With the increase of laser fluence, the relative amount of the fcc phase increases, and a maximum fraction is found at 100 mJ/cm^2 based on the observed peak intensity of the (200) reflection, which is the most intense XRD characteristic peak of the fcc phase. However, the diffracted intensity of the fcc phase decreases with further increase of laser fluence, and a notable drop in intensity is observed at 200 mJ/cm^2. This change of the fcc phase fraction is reasonable, because crystallization of the film occurs first with the increase of laser fluence, but then, melting and ablation of the film takes place with further increase of laser fluence, resulting in a reduction of the fcc phase fraction. These findings are consistent with the optical reflectivity results shown in Figure 1 and 2. Simultaneously, the Si(200) peak, which is the dominating peak of the as-deposited sample, gradually disappears due to the increased fraction of the crystalline fcc phase in the film covered on the Si substrate with the increase of laser fluence, and it appears again at 200 mJ/cm^2 due to the reduced fraction of the crystalline fcc phase by melting and ablation.

For comparison, crystallization of the films was also carried out by thermally annealing the films in high vacuum (1×10^{-4} Pa) at different temperatures (50–300 °C). The XRD results of those films (not shown here) show that transition

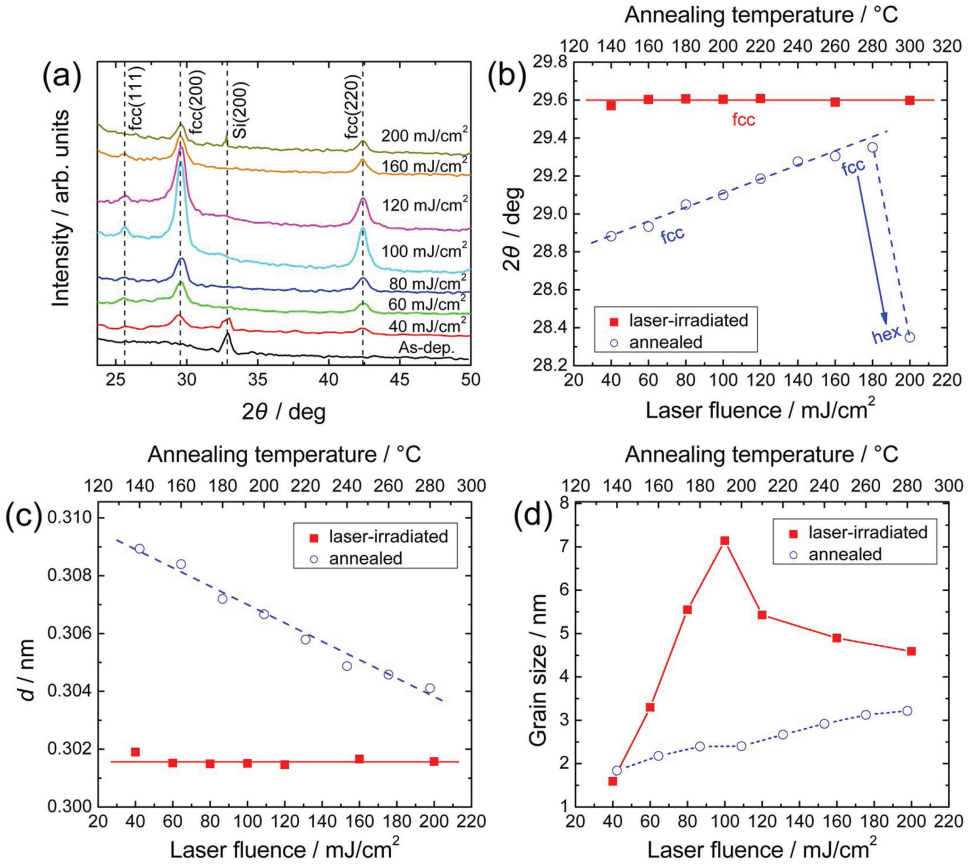

Figure 3. a) Evolution of XRD patterns of films with increasing laser fluence. b) 2θ position, c) corresponding $d_{(200)}$ value, and d) calculated grain size from the fcc (200) reflection as a function of laser fluence (denoted by red solid squares) and annealing temperature (denoted by blue open circles), respectively. The red solid lines and blue dashed lines in (b–d) are only intended as a guide for the eye.

from the amorphous to fcc and hexagonal phase occur at 140 and 300 °C, respectively. In addition, the crystalline phase fraction of annealed films increases with the increase of annealing temperature. Moreover, a large difference between the laser-irradiated and thermally annealed films is found that no hexagonal phase is formed in the laser-irradiated films, even for a high laser fluence (e.g., 160 mJ/cm^2), which is high enough to melt the films. The absence of the hexagonal phase in the laser-irradiated films is considered to be a consequence of the high heating rate (larger than 10^9 K/s) and short duration (20 ns) of the laser pulse. Generally, the phase transformation of a phase-change material is a thermally activated process. Energy barriers must be overcome when the material is transformed from the current phase to another phase. With increasing heating rate, the phase transformation temperatures (from amorphous to fcc, and fcc to hexagonal) are known to shift to higher temperatures.[27,28] The transformation temperature from fcc to the hexagonal phase was reported to be above the alloy melting temperature, when the heating rate approaches 1.7×10^8 K/s.[28] With even higher heating rate (>10^9 K/s) and short laser pulse duration as in our case, the phase transformation from fcc to hex is therefore effectively hindered.

A detailed analysis of the 2θ position of the (200) peak, which is the most intense XRD characteristic peak of the fcc phase, is depicted in Figure 3b. The 2θ position for the laser-irradiated films is in the range between 29.57° and 29.60°, almost keeping unchanged with increasing laser fluence. On the other hand, for the thermally annealed films, it is noted that the 2θ position increases from 28.83° to 29.34°, as the annealing temperature increases from 140 to 280°C, and subsequently decreases to 28.35° due to the phase transformation from fcc to hexagonal phase. Accordingly, the d value of the lattice plane (200) for the thermally annealed films (fcc phase), determined by $d_{(200)} = \frac{\lambda}{2\sin\theta}$, is found to be a function of annealing temperature, as indicated by the dashed line in Figure 3c. The d value starts from 0.309 nm at an annealing temperature of 140 °C and decreases to 0.304 nm at an annealing temperature of 280 °C. Dissimilarly, $d_{(200)}$ values of the laser-irradiated films nearly remain constant with the increase of laser fluence, showing an average value of 0.301 nm (see the solid line in Figure 3c). For bulk fcc GST, a $d_{(200)}$ value of 0.3013 nm is expected,[29] which is very close to those of the laser-irradiated films. The $d_{(200)}$ values of all the thermally annealed films with fcc structure are thus larger than those of the laser-irradiated films and the bulk one. This increase of $d_{(200)}$ values of the thermally annealed films is ascribed to the large tensile stress in the crystallized films.[5,30,31] It is known that the stress state of the film at room temperature depends on the creep at the annealing temperature, the difference in the coefficient of thermal expansion (CTE) of the film

and the substrate, and a potential plastic or brittle deformation during the cool-down.[30] During the heating of the GST films, it has been reported that the tensile stress is especially large at the onset of transformation from the amorphous to fcc phases due to the difference in the density of the two states.[30,32] This phase-change induced tensile stress is then reduced on further increase of the annealing temperature. During the cooling process, the crystalline GST film shows only elastic deformation and the stress progress in the tensile direction with a constant slope.[30,32] Therefore, the total tensile stress at room temperature, which sums up from the phase-change stress and the thermal stress, decreases with the increase of annealing temperature. Consequently, the largest $d_{(200)}$ value of 0.309 nm is found for the film with the largest tensile stress, when annealed at 140 °C. Further increase of the annealing temperature leads to a reduction of the total tensile stress in the film, resulting in the decrease of $d_{(200)}$ values with the increase of annealing temperature for the thermally annealed films.

Average grain size of the crystallized films, was estimated with the Scherrer formula using the full width at half maximum (FWHM) value of the (200) diffraction peak. As described in Figure 3d, the average grain size for the thermally annealed films ranges from 1.8 to 3.2 nm, and increases slightly with the increase of annealing temperature, while for the laser-irradiated films, the average grain size increases markedly from 1.6 to 7.1 nm with the increase of laser fluence from 40 to 100 mJ/cm^2. For even higher fluences, the average grain size decreases slightly due to the melting/ablation of films with further increase of laser fluence.

When comparing the XRD results with the reflectivity results shown in Figure 1b, a similar trend can be seen in that the fraction of the crystalline fcc phase increases with the increase of laser fluence up to 100 mJ/cm^2. In principle, the thicker the film, the higher laser fluence is needed to crystallize and amorphize the film. However, the highest fraction of the crystallized phase is observed at the same fluence of 100 mJ/cm^2, although two different film thicknesses are employed for the two kinds of measurements. This is caused by the heat loss for the thinner film owing to the following two factors. Firstly, the thermal diffusion length during the nanosecond pulse is about 60 nm,[10,33] much larger than the used film thickness (30 nm). Thus, the laser pulse penetrates the film, leading to the partial loss of laser energy. Secondly, the heat in the film induced by the laser pulse can be readily transferred from the film to the Si substrate due to the large thermal conductivity of Si and the thin thickness of the film. In addition, according to the optical reflectivity results shown in Figure 2, a complete amorphization occurs for the 30 nm thin film at a fluence of 160 mJ/cm^2. Following the same reasoning, amorphization will not occur for the 600 nm thick film, as evidenced by the XRD results in Figure 3a. A crystalline fcc phase can still be seen even at a high fluence (200 mJ/cm^2), which is high enough to melt the films. This is due to the fact that the laser-induced heat can not be quickly transferred from the film to Si substrate for such thick films. Thus, the melted film, which suffers a slow cooling rate, will transform to the crystalline fcc state after cooling.

Besides the optical reflectivity, another important quantity for the chalcogenide-based films is the film density. The density change upon crystallization produces considerable stress in the films,[30] which could be a potential reliability problem, especially for small-dimension electronic device cells. Therefore, it is of high significance to evaluate the film density change upon laser-induced crystallization. This density change can be determined from X-ray reflectivity (XRR) measurements. **Figure 4**a compares XRR curves of an as-deposited film and of the same film after laser irradiation at 100 mJ/cm^2. The visible film thickness related oscillations of the as-deposited film are clearly seen in the whole angular range, while the oscillations of the laser-irradiated film are more effectively attenuated at higher angles. Generally, with the increase of film roughness, a swifter decay of the oscillation amplitude is expected. Thus, an increase in film roughness upon laser irradiation can be concluded, which has also been confirmed with AFM measurements, see Supporting Information, Figure S1a–d. From the inset of Figure 4a, one can observe that the total reflection edge shifts towards a higher angle after laser irradiation. This indicates that the laser-irradiated film has a higher density than the as-deposited one since the critical angle (θ_c) for total reflection is proportional to the square root of density (ρ) as defined by the following equation

$$\theta_c = \lambda\sqrt{\frac{N_A r_0}{\pi}\frac{(f_0+f')}{A}\rho}$$

where λ, N_A, r_0, A and $(f_0 + f')$ are the wavelength of the used X-ray, Avogadro constant, Bohr radius, atomic mass and the atomic form factor, respectively.

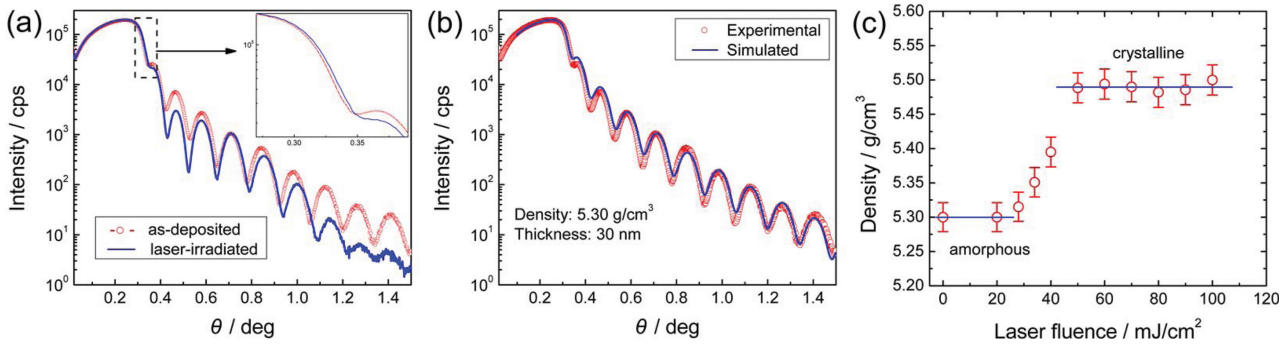

Figure 4. a) XRR measurements of a film before and after irradiation with a single laser pulse (100 mJ/cm^2). The inset shows the area around the total reflection edge. b) XRR measurement and the corresponding theoretical simulation of an as-deposited film. c) Density as a function of laser fluence for GST films obtained from XRR measurements.

Figure 4b shows the XRR measurement and the corresponding theoretical simulation of an as-deposited film. The thickness and density of the as-deposited film are determined to be 30 nm and 5.30 g/cm^3, respectively. More XRR measurements and the corresponding simulations were carried out for films irradiated with different fluences, and the obtained density as a function of laser fluence is shown in Figure 4c. The density maintains constant at fluences ≤20 mJ/cm^2. Above this fluence, an obvious density increase corresponding to the onset of a structural transformation is observed, in agreement with the optical reflectivity results shown in Figure 1b. With further increase of laser fluence from 50 to 100 mJ/cm^2, the density keeps almost unchanged within measurement error. The average densities of the as-deposited films and laser-induced crystalline films are decided to be 5.30 and 5.49 g/cm^3, respectively, corresponding to an increase of 3.58% in the density. Previous reports, which were mainly focused on the density changes induced by thermal annealing, have shown a density increase in the range from 5.78 to 6.80% upon annealing-induced crystallization of GST films from the amorphous to fcc states.[34,35] The density increase induced by laser irradiation in the present study is thus smaller than previously reported values induced by thermal annealing.

3. Conclusions

In summary, phase transformations in PLD-deposited GST films between amorphous and metastable fcc states have been induced by irradiation with a single nanosecond laser pulse. Two different phases were obtained by adjusting the laser fluence and could be distinguished by their different optical reflectivity. The effect of laser fluence on the crystalline nature of the films was studied. Large structural differences between the laser-irradiated and thermally annealed films were revealed. For the thermally annealed films, phase transition from amorphous to hexagonal structures occurred at 300 °C, and lattice distance $d_{(200)}$ values of the fcc phase decreased with the increase of annealing temperature. For the laser-irradiated films, the emergence of the hexagonal phase was not observed, and $d_{(200)}$ values of the fcc phase almost kept unchanged with the increase of laser fluence. These large differences were attributed to the high heating rate and short duration of the laser pulse. Furthermore, a change of density upon crystallization by laser irradiation was determined by XRR measurements, showing an increase of 3.58% in the density.

4. Experimental Section

GST films were grown on Si substrates by pulsed laser ablation of a $Ge_2Sb_2Te_5$ ceramic target using a KrF excimer laser (LPXpro240). The laser was operated with the following parameters: wavelength of 248 nm, pulse duration of 20 ns, repetition rate of 10 Hz, and laser fluence on the target of 1.5 J/cm^2. The working pressure was 5×10^{-5} Pa during deposition. Si substrates were dipped in hydrofluoric acid and subsonically cleaned in deionized water and ethanol. The cleaned substrates were positioned parallel to the target surface at a target-substrate distance of 6.6 cm. Both target and substrates were rotated in order to avoid damage of the target and to improve the thickness homogeneity of the films, respectively. Using the above mentioned parameters, two types of samples with thickness of 30 and 600 nm were prepared.

Single shot pulsed laser irradiation was performed on the GST films in order to induce local phase changes. The laser beam from the KrF excimer laser was focused by a convex lens on the surface of GST films using a single nanosecond laser pulse (20 ns). The spot size of the laser beam was about 4 × 6 mm^2 and the laser fluence was varied between 20 and 300 mJ/cm^2 by adjusting the laser pulse energy. The fluence is defined as laser pulse energy/area of spot size in the units of mJ/cm^2.

For comparison, the as-deposited films were also crystallized by thermal annealing. The annealing was carried out in high vacuum (1×10^{-4} Pa) at different temperatures (50–300 °C) for 20 min.

The surface of the films before and after laser irradiation was examined by field emission scanning SEM and AFM. The optical reflectivity of the films was recorded using an UV/Vis spectrophotometer with a wavelength range from 350 to 800 nm. Crystal structure analysis of the laser-irradiated and thermal-annealed films was carried out by XRD using monochromized Cu $K\alpha$ radiation ($\lambda = 0.15406$ nm) in $\theta/2\theta$ scans. The film density and thickness changes upon laser-induced crystallization were obtained from XRR measurements.

Supporting Information

Supporting Information is available from the Wiley Online Library or from the author.

Acknowledgements

This work has been supported by the Leipzig School of Natural Sciences BuildMoNa (Grant No. GS 185/1), the European Social Fund (ESF) within the Nachwuchsforschergruppe "Multiscale functional structures", and the National Natural Science Foundation of China (Grant No. 11105047).

Received: September 14, 2012
Revised: December 20, 2012
Published online: February 25, 2013

[1] M. Wuttig, N. Yamada, *Nat. Mater.* **2007**, *6*, 824.
[2] A. V. Kolobov, P. Fons, A. I. Frenkel, A. L. Ankudinov, J. Tominaga, T. Uruga, *Nat. Mater.* **2004**, *3*, 703.
[3] M. H. R. Lankhorst, B. Ketelaars, R. A. M. Wolters, *Nat. Mater.* **2005**, *4*, 347.
[4] P. Nemec, A. Moreac, V. Nazabal, M. Pavlista, J. Prikryl, M. Frumar, *J. Appl. Phys.* **2009**, *106*, 103509.
[5] H. B. Lu, E. Thelander, J. W. Gerlach, D. Hirsch, U. Decker, B. Rauschenbach, *Appl. Phys. Lett.* **2012**, *101*, 031905.
[6] B. Liu, Z. T. Song, S. L. Feng, B. Chen, *Chin. Phys. Lett.* **2004**, *21*, 1143.
[7] T. Gotoh, K. Kawarai, *Phys. Status Solidi A-Appl. Mater.* **2010**, *207*, 639.
[8] I. Friedrich, V. Weidenhof, W. Njoroge, P. Franz, M. Wuttig, *J. Appl. Phys.* **2000**, *87*, 4130.
[9] M. H. Jang, S. J. Park, S. J. Park, M. H. Cho, E. Z. Kurmaev, L. D. Finkelstein, G. S. Chang, *Appl. Phys. Lett.* **2010**, *97*, 152113.
[10] J. Siegel, W. Gawelda, D. Puerto, C. Dorronsoro, J. Solis, C. N. Afonso, J. C. G. de Sande, R. Bez, A. Pirovano, C. Wiemer, *J. Appl. Phys.* **2008**, *103*, 023516.
[11] H. Y. Cheng, S. Raoux, Y. C. Chen, *J. Appl. Phys.* **2010**, *107*, 074308.
[12] G. J. Zhang, D. H. Gu, X. W. Jiang, Q. X. Chen, F. X. Gan, *Appl. Surf. Sci.* **2006**, *252*, 4083.

[13] J. Siegel, A. Schropp, J. Solis, C. N. Afonso, M. Wuttig, *Appl. Phys. Lett.* **2004**, *84*, 2250.
[14] J. Kong, S. J. Wei, Z. B. Wang, G. H. Li, J. Li, *J. Infrared Millimeter Waves* **2011**, *30*, 6.
[15] H. J. Sun, L. S. Hou, Y. Q. Wu, J. S. Wei, *J. Non-Cryst. Solids* **2008**, *354*, 5563.
[16] H. J. Sun, L. S. Hou, X. S. Miao, Y. Q. Wu, *Rare Metal Mater. Eng.* **2010**, *39*, 377.
[17] R. Y. Kim, H. G. Kim, S. G. Yoon, *Appl. Phys. Lett.* **2006**, *89*, 102107.
[18] E. Morales-Sanchez, E. F. Prokhorov, J. Gonzalez-Hernandez, A. Mendoza-Galvan, *Thin Solid Films* **2005**, *471*, 243.
[19] D. J. Milliron, S. Raoux, R. Shelby, J. Jordan-Sweet, *Nat. Mater.* **2007**, *6*, 352.
[20] M. Xu, S. J. Wei, S. Wu, F. Pei, J. Li, S. Y. Wang, L. Y. Chen, *J. Korean Phys. Soc.* **2008**, *53*, 2265.
[21] P. K. Khulbe, T. Hurst, M. Horie, M. Mansuripur, *Appl. Opt.* **2002**, *41*, 6220.
[22] S. Choi, B. J. Choi, T. Eom, J. H. Jang, W. Lee, C. S. Hwang, *J. Phys. Chem. C* **2010**, *114*, 17899.
[23] V. Weidenhof, I. Friedrich, S. Ziegler, M. Wuttig, *J. Appl. Phys.* **2001**, *89*, 3168.
[24] K. Zhang, S. M. A. Li, G. F. Liang, H. Huang, Y. Wang, T. S. Lai, Y. Q. Wu, *Physica B* **2012**, *407*, 2447.
[25] H. S. Carslaw, J. C. Jaeger, *Conduction of Heat in Solids*, Oxford Science Publication, Oxford **2008**.
[26] D. Bäuerle, *Laser Processing and Chemistry*, Springer, Berlin **2000**.
[27] J. Orava, A. L. Greer, B. Gholipour, D. W. Hewak, C. E. Smith, *Nat. Mater.* **2012**, *11*, 279.
[28] D. Y. Chiang, T. R. Jeng, D. R. Huang, Y. Y. Chang, C. P. Liu, *Jpn. J. Appl. Phys.* **1999**, *38*, 1649.
[29] N. Yamada, T. Matsunaga, *J. Appl. Phys.* **2000**, *88*, 7020.
[30] I. M. Park, J. K. Jung, S. O. Ryu, K. J. Choi, B. G. Yu, Y. B. Park, S. M. Han, Y. C. Joo, *Thin Solid Films* **2008**, *517*, 848.
[31] S. N. Song, Z. T. Song, L. C. Wu, B. Liu, S. L. Feng, *J. Appl. Phys.* **2011**, *109*, 034503.
[32] T. P. L. Pedersen, J. Kalb, W. K. Njoroge, D. Wamwangi, M. Wuttig, F. Spaepen, *Appl. Phys. Lett.* **2001**, *79*, 3597.
[33] J. Siegel, A. Schropp, J. Solis, C. N. Afonso, M. Wuttig, *Appl. Phys. Lett.* **2004**, *84*, 2250.
[34] M. Wuttig, R. Detemple, I. Friedrich, W. Njoroge, I. Thomas, V. Weidenhof, H. W. Woltgens, S. Ziegler, *J. Magn. Magn. Mater.* **2002**, *249*, 492.
[35] K. Wang, C. Steimer, D. Wamwangi, S. Ziegler, M. Wuttig, *Appl. Phys. A-Mater. Sci. Process.* **2005**, *80*, 1611.